

1 **DEM-based analysis of earthquake-induced shallow landslide**
2 **susceptibility**

3 Shuichi Hasegawa. Ranjan Kumar Dahal* . Toshiaki Nishimura. Atsuko Nonomura. Minoru
4 Yamanaka.

5 S. Hasegawa

6 *Dept. of Safety Systems Construction Engineering, Faculty of Engineering, Kagawa*
7 *University, 2217-20, Hayashi-cho, Takamatsu City, 761-0396, Japan*

8 R. K. Dahal^{1, 2*} . A. Nonomura¹ . M. Yamanaka¹

9 *1 Dept. of Safety Systems Construction Engineering, Faculty of Engineering, Kagawa*
10 *University, 2217-20, Hayashi-cho, Takamatsu City, 761-0396, Japan*

11 *2 Department of Geology, Tri-Chandra Multiple Campus, Tribhuvan University, Ghantaghar,*
12 *Kathmandu, Nepal*

13

14 T. Nishimura

15 *Fukken Co. Ltd., 2-10-11 Hikarimachi, Higashi-ku, Hiroshima, 732-0052, Japan*

16

17 *Corresponding author

18 Phone: 0081-87-864-2145

19 Fax: 0081-87-864-2031

20 Email: ranjan@ranjan.net.np

21

22 **Abstract**

23 This paper describes a simple method of Digital Elevation Model (DEM)-based earthquake-induced shallow
24 landslide susceptibility analysis. Considering topographic effects in amplification of earthquake ground motion,
25 Uchida et al. (2004) have developed a topographical parameter based empirical description of landslide
26 susceptibility during an earthquake. In this research, the method proposed by Uchida et al. (2004) was utilized in
27 raster GIS and shallow landslide susceptibility analysis was performed in the study area of Nishiyama Town of
28 Kashiwazaki City, Niigata prefecture, Japan. The correlation of shallow landslides generated by the Niigataken
29 Chuetsu-oki Earthquake in 2007 with landslide susceptibility values suggests that the method proposed by
30 Uchida et al. (2004) can be more than 78.14% accurate in delineating the probable locations of earthquake-
31 induced landslides. By calibrating landslide data and landslide susceptibility values in a small site within the
32 study area, a final landslide susceptibility map was prepared for the whole study area. The resultant susceptibility
33 map is very useful for regional scale planning.

34 **1 Introduction**

35 Earthquake-induced landslides are one of the most damaging natural disasters. Commonly,
36 damage from earthquake-induced landslides is worse than damage related to the shaking and
37 rupture of the earthquake itself. Earthquake-induced landslides damage and destroy homes
38 and other structures, block roads, destroy utilities, and dam up river and streams. In recent
39 years, Geographic Information Systems (GIS) and remote sensing have significantly
40 improved our ability to map earthquake-induced landslides. With the application of aerial
41 photographs and field verifications, landslides induced by earthquakes have been mapped and

42 analyzed in California, El Salvador, Taiwan, Japan, Italy and Pakistan (e.g., [Wilson and](#)
43 [Keefer 1985](#); [Harp and Keefer 1990](#); [Harp and Jibson 1996](#); [Jibson et al. 2000](#); [Parise and](#)
44 [Jibson 2000](#), [Capolongo et al. 2002](#); [Wang et al. 2002, 2003](#); [Chigira et al. 2003](#); [Chigira and](#)
45 [Yagi 2006](#); [Wang et al. 2007](#); [Owen et al. 2008](#)). Several methods have been developed for
46 the evaluation of hazards represented by earthquake-induced landslides, including statistical
47 analysis ([Keefer 1984, 2000](#); [Lee and Evangelista 2006](#)) and a deterministic method
48 ([Mankelov and Murphy 1998](#); [Van Westen and Terlien 1996](#); [Jibson et al. 1998, 2000](#); [Luzy](#)
49 [and Pergalain 1996, 2000](#); [Carro et al. 2003](#)), both of which aim to quantify earthquake-
50 induced landslide susceptibility and hazard zonation. In the deterministic method, most of the
51 work has used the pseudo-static method or the Newmark cumulative displacement method
52 ([Newmark, 1965](#)). [Mankelov and Murphy \(1998\)](#) have suggested that the cumulative
53 displacement method proved most successful at predicting the location of shallow unstable
54 slopes. However, deterministic methods rely on having access to detailed information, such as
55 strength parameters and sliding depth, which are not readily available in many cases. Some
56 studies have also focused on general correlations between earthquake-induced landslide
57 occurrence and slope steepness, distance from the earthquake's source, or underlying geologic
58 units ([Keefer 2000](#); [Khazai and Sitar 2003](#); [Chigira and Yagi 2006](#); [Wang et al. 2007](#)). These
59 studies have provided valuable information about the characteristics of earthquake-induced
60 landslides.

61 The effects of topography on earthquake ground motion are also well documented. Two types
62 of findings have motivated studies of the effect of the topography on seismic waves. The
63 earliest investigations showed that topographic features are basically responsible for
64 dissipation of energy (e.g. [Gilbert and Knopoff, 1960](#); [Greenfield, 1971](#)). Later observations
65 noted extremely high accelerations at sites located on topographic ridges (e.g. [Davis and West](#)
66 [1973](#); [Trifunac 1973](#); [Bannister et al. 1990](#); [Griffith and Bolinger 1979](#); [Ohtsuki and Harumi](#)
67 [1983](#); [Umeda et al. 1986](#); [Geli et al. 1988](#); [Kawase and Aki 1990](#); [Clouser and Langston 1995](#);
68 [Ambraseys and Srbulov 1995](#); [Bouchan et al. 1996](#); [Chávez-García et al. 1996](#); [Miles and](#)
69 [Keefer 2000](#); [Gazetas et al. 2002](#); [Lin et al. 2003](#)). Observations of the damage patterns of
70 earthquakes, such as the 1987 Whittier Narrows, California earthquake, the 1989 Loma Prieta
71 (California) earthquake, the 1994 Northridge, California earthquake, the 1999 Chi-Chi
72 earthquake of Taiwan, the 2004 Chuetsu earthquake of Niigata Prefecture, Japan, and the
73 2005 Kashmir earthquake of Pakistan also indicate the occurrence of intense shaking in
74 elevated areas of rugged topography. [Geli et al. \(1988\)](#) have reported that buildings on crests
75 suffer more damage than those located at the base and they conclude that there is always
76 significant amplification of frequencies corresponding to wavelengths about equal to
77 mountain width at hilltops with respect to the base. Similarly, an amplification-
78 deamplification pattern on slopes leads to a strong energy differential on the upper part of the
79 slope. For the case of the Chi-Chi earthquake, [Lin et al. \(2003\)](#) mentioned that landslide
80 frequency is much higher on or near the crests of hills. Field experiments by [Chávez-García et](#)
81 [al. \(1996\)](#) indicate that a topographic site amplification effect does exist and the amount of
82 amplification depends on the frequency at the site location. [Bouchon et al. \(1996\)](#) have also
83 confirmed that amplifications of seismic energy occur at and near the top of hills (defined as
84 elongated elliptical shapes with an aspect ratio of 2-to-1) over a broad range of frequencies.

85 Many models exist for assessing the stability of slopes during earthquakes. These models
86 have been used to assess the stability of individual slopes and have been incorporated into
87 landslide potential assessments. Traditionally, landslide potential has been analyzed by
88 applying deterministic and static stability models. Both intrinsic and extrinsic parameters are
89 used for analysis. The intrinsic variables include bedrock geology, geomorphology, soil depth,
90 soil type, slope gradient, slope aspect, slope curvature, elevation, engineering properties of the
91 slope material, land use patterns, and drainage patterns. Extrinsic variables include heavy
92 rainfall, earthquakes, and volcanoes. Observations and experience show that the probability of
93 landslide occurrence depends on both intrinsic and extrinsic variables. However, extrinsic
94 variables are site specific and possess a temporal distribution. The intrinsic parameters used in
95 analysis usually have many restrictions and have a wide range of variability in terms of
96 geotechnical index value. As a result, deterministic assessments always contain some
97 limitations. To overcome this issue, in this work, only DEM-based intrinsic parameters (slope
98 gradient and slope curvature) and one extrinsic parameter (an earthquake) were used within
99 the geographical information system (GIS) for the analysis of landslide susceptibility.
100 Motivated by findings regarding the effects of topography on the amplification of earthquake
101 ground motion, [Uchida et al. \(2004\)](#) have developed a topographical parameter-based
102 empirical relationship for landslide analysis during an earthquake. In this research, the method
103 proposed by Uchida et al. (2004, 2006) was utilized within the GIS platform and landslide
104 susceptibility analysis was performed. The main objective of this paper is to investigate the
105 landslide susceptibility of an earthquake-prone area using the methodology described by
106 Uchida et al. (2004). For this purpose, the Kashiwazaki area, which experienced several
107 landslides after the Niigataken Chuetsu-oki Earthquake in 2007, was selected as the study
108 area.

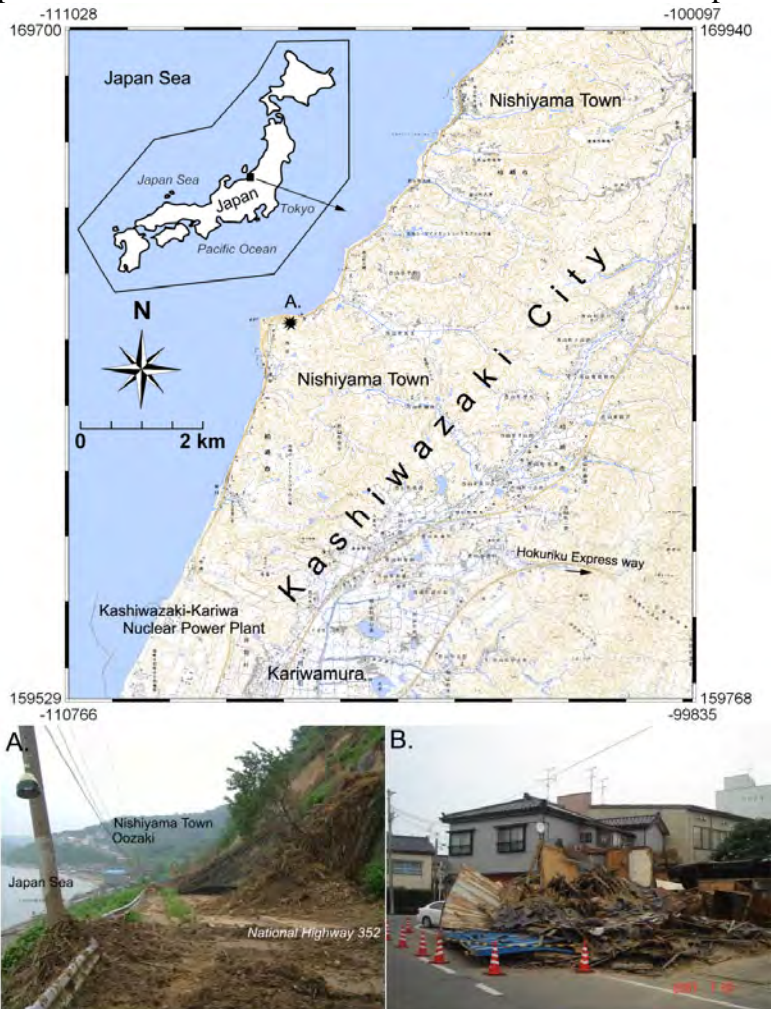
109 **2 The study area**

110 **2.1 Geological and tectonic setting**

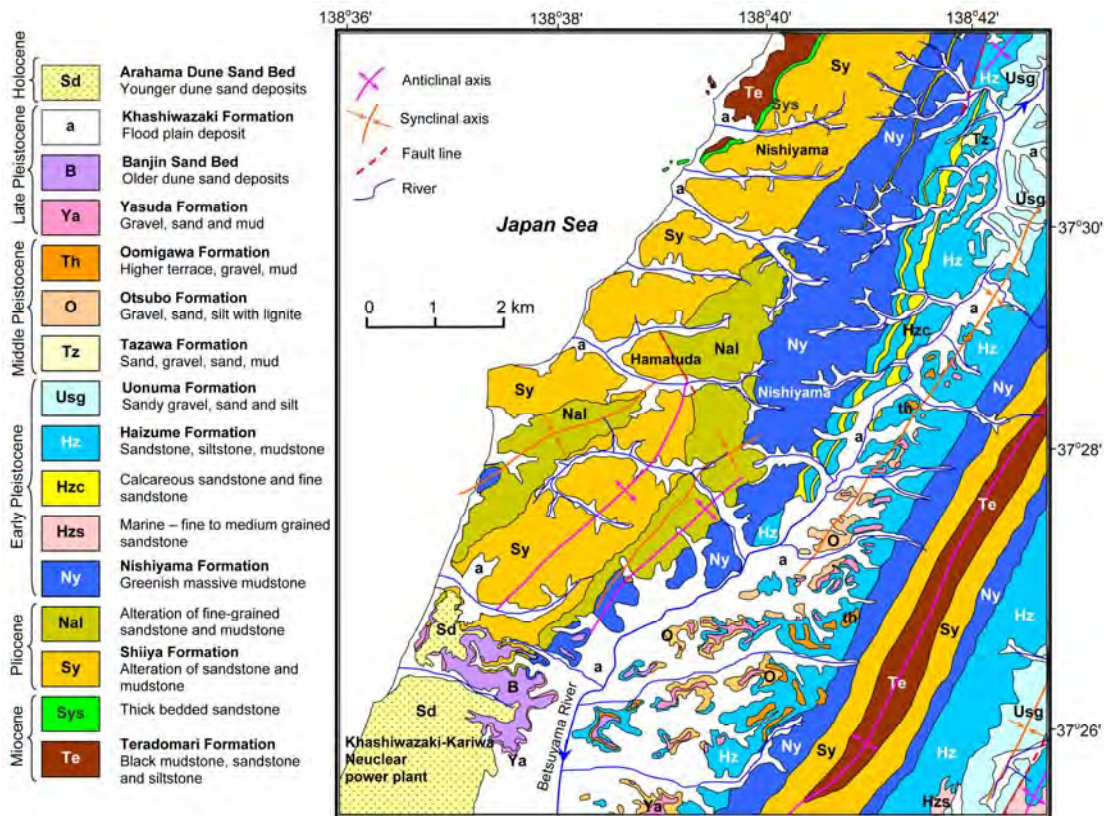
111 The Japanese archipelago is comprised of five main island arcs extending approximately 3000
112 km in the north-south direction and encompasses a total area of about 378,000 square km. The
113 five main island arcs are, from north to south, Kurile Arc, Northeast Honshu Arc, Izu-Mariana
114 Arc, Southwest Honshu Arc and Ryukyu Arc. These arcs approximately represent plate
115 boundaries between the North American Plate, Pacific Plate, Eurasian Plate, and Philippine
116 Sea Plate ([GSJ, 2002](#)). Because of this arc-plate relationship, Japan is located in an area of
117 severe crustal movement, and is within one of the world's most seismically active regions. As
118 a result, Japan faces tremendous problems from earthquake-induced landslides. Tectonically,
119 Niigata region is situated on a zone of compressional deformation that is associated with the
120 boundary between the Eurasian and the North American plates ([GSJ, 2002](#)).

121 The area of study in this research is situated in the northern part of Kashiwazaki city, which
122 was heavily affected by the Niigataken Chuetsu-oki Earthquake in 2007. Geographically, the
123 area lies between 37°26'5" and 37°31'29" North and between 138°34'35" and 138°42'25" East.
124 The area includes Nishiyama town and the adjacent area as well as the northern portion of the
125 Kashiwazaki-Kariwa nuclear power plant, which was partly damaged by the Niigataken
126 Chuetsu-oki Earthquake in 2007. The study area, shown in [Fig. 1](#), was chosen for several

127 reasons. First, the Niigataken Chuetsu-oki Earthquake triggered many landslides in this area,
 128 so it has sufficient recent data on earthquake-triggered landslides. Second, there are good
 129 quality aerial photos available that were taken immediately after the Niigataken Chuetsu-oki
 130 Earthquake, facilitating the location of all landslides. Third, the mountain located within this
 131 study area has features typically associated with seismic energy amplification.
 132 The study area consists primarily of hills of sedimentary rock with a small amount of igneous
 133 rock (Takeuchi et al. 2007). The southern portion of the study area (around the Kashiwazaki-
 134 Kariwa nuclear power plant) consists of the Arahama Dune Bed. Mudstone and sandstone of
 135 the early Pliocene Teradomari Formation are distributed in the north and southeast parts of the
 136 study area with sporadic rhyolitic tuff. The central part of the study area consists primarily of
 137 massive sandstone, siltstone and interbedded sandstone and siltstone of the late Pliocene
 138 Nishiyama Formation (Kobayashi et al. 1993; Kobayashi et al. 1995). The Betsuyama River
 139 flows from north to south through the middle part of the study area. The bedrock is blanketed
 140 locally by colluvium, and unconsolidated Pleistocene to Holocene alluvial deposits are
 141 present within river and stream channels and their floodplains (Fig. 2).



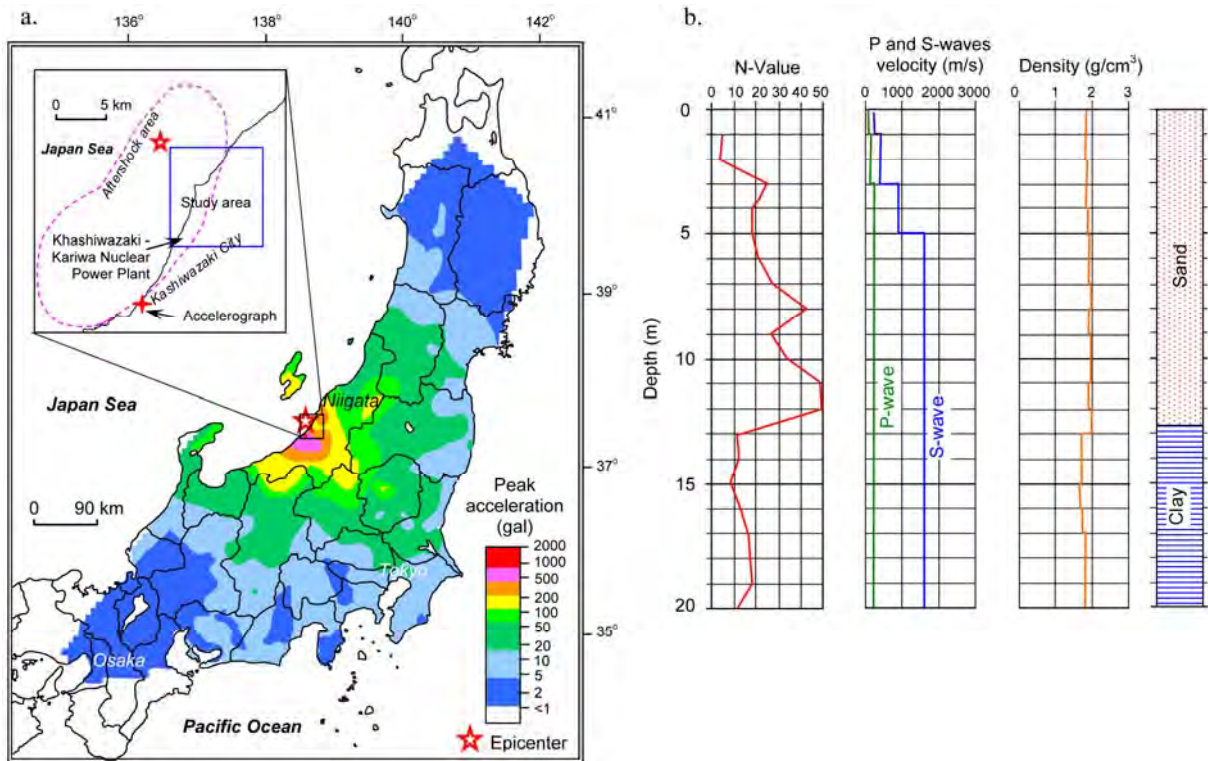
142
 143 Figure 1. Map of study area (top). Photograph A shows the problems of landslides and road
 144 damage on National Highway 352, and photograph B shows a damaged house in Kashiwazaki
 145 city. The location of photograph A is shown on the map. (Source of topographic map: GSI,
 146 2007)



147
 148 Figure 2. Geologic map of the study area (modified after Kobayashi et al. 1993 and
 149 Kobayashi et al. 1995).

150 2.2 Niigatoken Chuetsu-oki Earthquake

151 The Niigata Prefecture in central Japan was hit by two major earthquakes in this decade. On
 152 23 October 2004 the Chuetsu earthquakes induced a large number of landslides, causing
 153 severe damage and isolating villages located in mountainous areas. At 10:13 am on 16 July
 154 2007, another strong earthquake hit the Kashiwazaki area (Fig. 3). Subsequently, many
 155 earthquake-induced landslides caused severe damage to roads, railways, and houses. The
 156 Japan Meteorological Agency (JMA) named this earthquake the Niigatoken Chuetsu-oki
 157 Earthquake and recorded its magnitude as 6.8. According to the USGS, the movement
 158 magnitude of this earthquake was 6.6 (Kayen et al. 2007). The earthquake epicenter was
 159 situated on continental shelf of the Japan Sea at 138.6° East and 37.5° North and about 20 km
 160 northwest of the Kashiwazaki-Kariwa nuclear power plant. JMA estimated the depth of the
 161 epicenter to be approximately 17 km (JMA, 2007). This earthquake was felt throughout the
 162 Niigata and Toyama prefectures.



163
 164 Figure 3. (a) Earthquake intensity map of the Niigataken Chuetsu-oki Earthquake in 2007.
 165 The Kashiwazaki area experienced the highest ground acceleration: 813 gal. The location of
 166 the accelerograph in Kashiwazaki city is shown in the inset. (b) Borehole log of ground
 167 acceleration measurements (at the accelerograph site). The unit of density is $1 \text{ g/cm}^3 = 9.81$
 168 kN/m^3 . Figure 3a is modified after [K-Net \(2008\)](#) and Figure 3b is modified after [Tobishima](#)
 169 [Corporation \(2008\)](#).

170 At Kashiwazaki city, ground acceleration exceeding 813 gal was observed during the
 171 Niigataken Chuetsu-oki Earthquake (Fig. 3). This value was measured on the Kashiwazaki
 172 Formation (flood plain deposit, see Fig. 2). A borehole log of the measurement site is shown
 173 in Fig. 3b. The quake affected an approximately 100-km-wide area along the coastal areas of
 174 Kashiwazaki City. Analysis of waveforms from source inversion studies indicates that the
 175 event occurred along a thrust fault with a NE trend ([Kayen et al., 2007](#)). The fault plane is
 176 either a strike of 34 degrees with a dip of 51 degrees or a strike of 238 degrees with a dip of
 177 41 degrees ([ERI, 2007](#)). Which of these two planes is associated with the main shock rupture
 178 is unresolved, but the attenuation relationship analysis indicates that the northwest-dipping
 179 fault is the most probable one ([Kayen et al. 2007](#)).

180 A total of 15 people were killed by this earthquake, and more than 400 people were injured. In
 181 addition, extensive damage occurred in houses, roads, highways and the power plant. Many
 182 landslides occurred in the Nishiyama town area of Kashiwazaki and blocked roads and
 183 railways ([Fig. 4](#)). A few large-scale landslides also occurred along the national highway of
 184 Nishiyama and the adjacent area.



185
 186 Figure 4. Landslide at the Oomigawa Train Station on the Shinetsu. This was among the
 187 largest of the coastal landslides to the south of Kashiwazaki. Many more landslides were
 188 observed to the north and south of this location. Earthquake damage was also observed on
 189 buildings in this location. The roofs of earthquake-damaged houses were covered by plastic
 190 sheets.

191 **3 DEM-based earthquake-induced landslide analysis**

192 The method proposed by Uchida et al. (2004, 2006) was used in this study to perform an
 193 earthquake-induced landslide susceptibility analysis within the GIS platform. Taro Uchida
 194 and his team extensively studied landslide damage in the Rokko mountain region (granitic
 195 terrain) after the Hanshin-Awaji Earthquake (Kobe earthquake) of 1995. They derived a
 196 landslide probability function based on discriminant analysis using slope, average curvature
 197 and maximum ground acceleration (Uchida et al. 2004, 2006) without considering geology
 198 and other intrinsic factors. Previously, Nishida et al. (1997) also noted that slope and average
 199 curvature are very important parameters for quantifying earthquake-induced landslide
 200 potential.

201 Uchida et al. (2004) defined average curvature as the average of the maximum and minimum
 202 curvatures of all geodesics on the curved slope. In raster GIS, the average curvature, ε , can be
 203 derived from the following relationship:

204
$$\varepsilon = \frac{\frac{\partial^2 f}{\partial x^2} \left\{ 1 + \left(\frac{\partial f}{\partial y} \right)^2 \right\} + \frac{\partial^2 f}{\partial y^2} \left\{ 1 + \left(\frac{\partial f}{\partial x} \right)^2 \right\} - 2 \frac{\partial f}{\partial x} \frac{\partial f}{\partial y} \frac{\partial^2 f}{\partial x \partial y}}{\sqrt{2 \left(1 + \left(\frac{\partial f}{\partial x} \right)^2 + \left(\frac{\partial f}{\partial y} \right)^2 \right)^3}} \dots \dots \dots (1)$$

205 where f is the pixel value of a DEM generated from the contour map and x and y are the local
 206 coordinates. Concave slope gives a positive curvature value and convex slope gives a negative
 207 curvature value. On the basis of average curvature defined in Eq. (1), Uchida et al. (2004)
 208 derived the landslide probability function from discriminant analysis as follows:

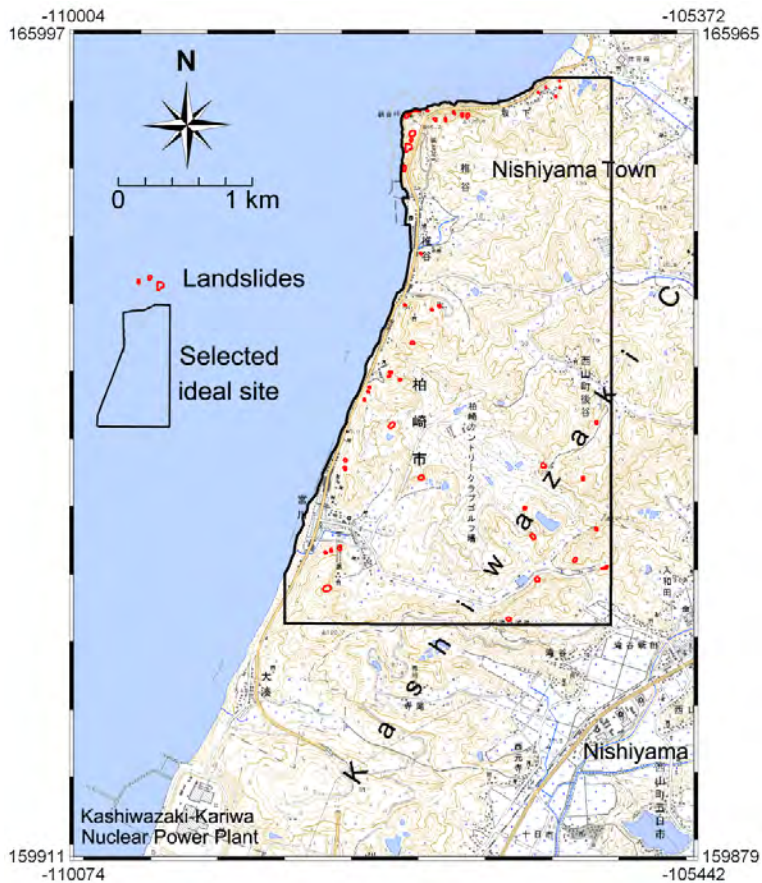
209
$$F = 0.075[\theta] - 8.9[\varepsilon] + 0.0056[a_{\max}] - 3.2 \dots \dots \dots (2)$$

210 where F is the landslide probability function or discriminant score, θ is the slope angle in
211 degrees, ε is the average curvature, and a_{\max} is the maximum ground acceleration in gal (1 gal
212 = 0.01 m/s²). Pixels having positive F -value always have the potential to fail during an
213 earthquake, and negative F -values suggest the slope will not fail during an earthquake.
214 Equations (1) and (2) are easily applicable to DEM in the GIS platform.
215 Uchida et al. (2006) have tested the applicability and predictive power of F -values for the
216 earthquake-induced landslides of Kozushima Island (on July 1, 2000) and the Niigata-ken
217 Chuetsu Earthquake of October 23, 2004. Kozushima Island consists of volcanic rocks and
218 the Niigata area consists of sedimentary rocks. They developed similar discriminant equations
219 for the Kozushima Island Earthquake and the Niigata-ken Chuetsu Earthquake. When
220 discriminant scores (F -value) of the Kozushima Island Earthquake (volcanic rock terrain) and
221 the Niigata-ken Chuetsu Earthquake (sedimentary rock terrain) were tested with discriminant
222 scores from Eq. 2 (Rokko mountain region, granitic rock terrain), they noticed that
223 discriminant scores were almost identical (Uchida et al., 2006). This analysis of Uchida et al.
224 (2006) also proved that the method was a useful tool for assessing the relative potential of
225 shallow landslides triggered by earthquakes even without consideration of site geology.
226 Similarly, when Uchida et al. (2006) correlated discriminant scores (F -values) with deep-
227 sheeted earthquake-induced landslides, they could not obtain satisfactory results. Thus Eq. 2
228 is not an effective tool for predicting the location of deep-sheeted earthquake-induced
229 landslides.

230 **4 Landslide inventory map**

231 Developing an accurate landslide inventory map is a primary component of landslide
232 susceptibility mapping. In the study area, only the area around the Kashiwazaki-Kariwa
233 nuclear power plant has good coverage by recent aerial photos. The photos include the coastal
234 parts of Kashiwazaki City and Nishiyama town. They were taken and distributed by the
235 Geographical Survey Institute, Japan, immediately after the Niigataken Chuetsu-oki
236 Earthquake of 2007. Thus, for the purpose of accurate landslide mapping, Nishiyama town
237 was selected as an ideal sub-site within the study area. It covers about 7.4 square km of the
238 coastal side of Nishiyama town (Fig. 5).

239 For the selected sub-site, landslide inventory mapping was performed with aerial color
240 photographs and stereoscopic images. A landslide inventory map was prepared from a
241 topographical base map with a 1:25000 scale. There was a significant chance that the
242 landslides visible in recent aerial photographs could include both old rainfall-induced
243 landslides and new earthquake-induced landslides from the Niigataken Chuetsu-oki
244 Earthquake. Thus, to verify that the landslides were earthquake-induced and to correct the
245 inventory map, fieldwork was carried out on July 26 to 29, 2007 to observe the landslide scars.
246 All landslide sites were visited and errors were corrected in the inventory map. Rainfall-
247 induced landslides were removed from the inventory map and a final inventory map of
248 earthquake-induced landslides was prepared for analysis. Most of the landslides had failure
249 depths of less than 2 m, and translational movement was evident on the failure plain. The
250 scarp length of the landslides ranged from 10.8 m to 47.6 m with mean 22.3 m and standard
251 deviation 9 m. The final inventory map is given in Fig. 5.



252
 253 Figure 5. Sub-site selected from study area for landslide inventory mapping and detailed field
 254 study. (Source of topographic map: GSI, 2007)

255 **5 Data analysis**

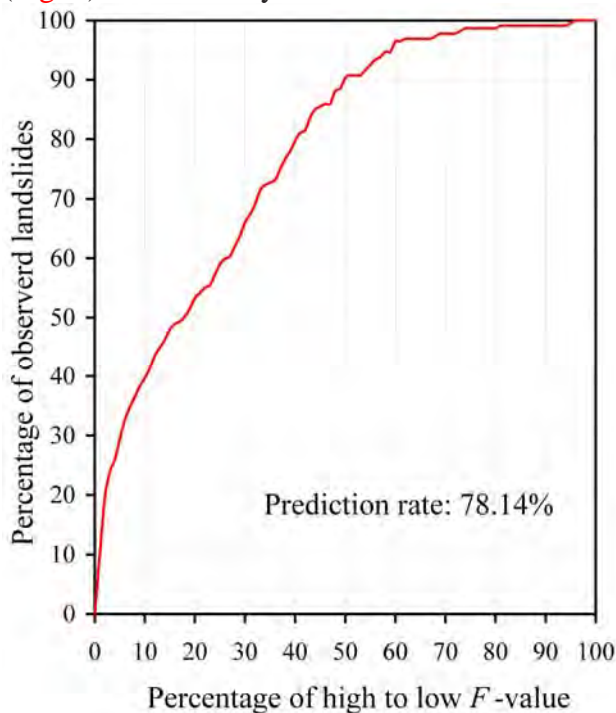
256 Our methodology for landslide susceptibility mapping consisted of data collection and
 257 construction of a spatial database from which relevant factors were extracted, followed by
 258 assessment of the landslide susceptibility using the relationship between existing landslide
 259 and susceptibility maps, with subsequent validation of results. A key feature of this approach
 260 is that the probability of landslide occurrence is comparable to the rate of occurrence of
 261 observed landslides.

262 For this study, a thematic data layer of slope and average curvature were prepared in GIS.
 263 DEM data (10 m x 10 m pixel) purchased from Hokkaido-Chizu Co. Ltd. were considered as
 264 basic data sources to generate these layers. GIS software ILWIS 3.3 (ITC, 2006) was used.
 265 ILWIS 3.3 has a built-in command for slope calculation and Eq. (1) was used for the average
 266 curvature calculation. As per the data provided by JMA, the maximum ground acceleration
 267 value of 813 gal was used (based on the Niigatoken Chuetsu-oki Earthquake-related ground
 268 acceleration measured at Kashiwazaki city, see Fig. 3) and the landslide susceptibility index
 269 (F -value) was determined from Eq. (2). Finally, a spatial distribution of F -values was
 270 prepared in GIS raster.

271 **6 Preparation of susceptibility map**

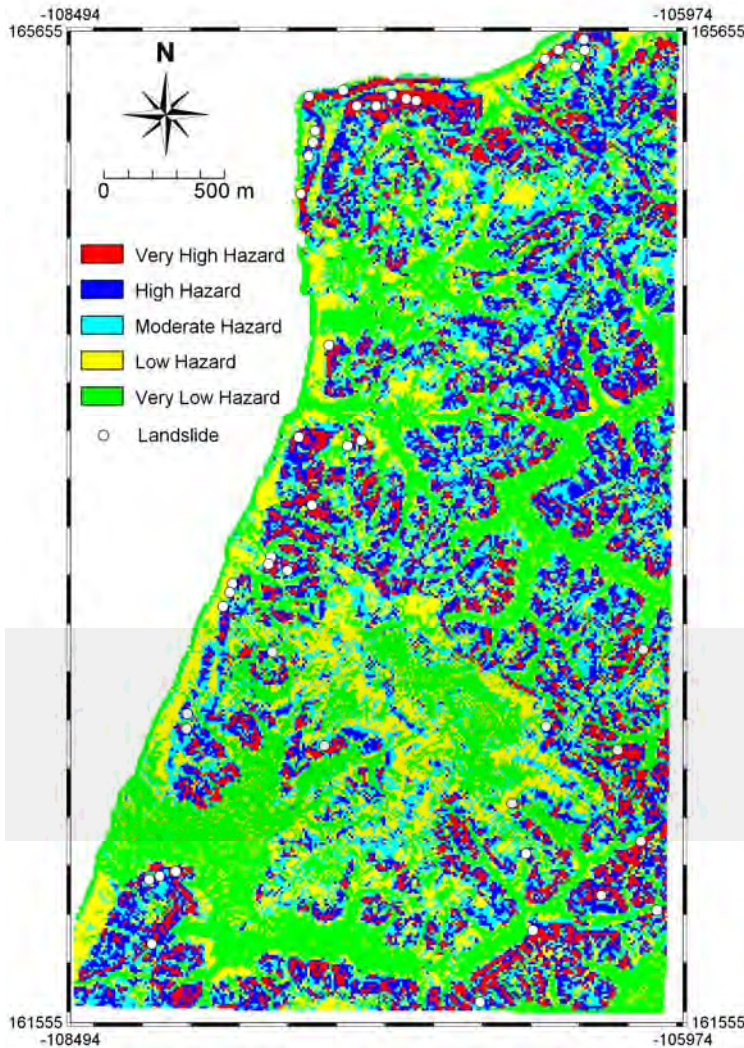
272 The calculated F -value for the selected sub-site does not have any correlation with the
 273 earthquake-induced landslides in the area. To overcome this issue and to check the predictive

274 power of F for landslide occurrence, the F -values were qualitatively examined with the help
 275 of success rate curves. In statistical landslide susceptibility analysis, the success rate is a
 276 measure of goodness of fit (Chung and Fabbri 1999; Van Westen et al. 2003; Lee, 2004;
 277 Dahal et al., 2008a, 2008b; Kamp et al. 2008) and for this research, success rate can be a
 278 measure of the predictive power of landslide susceptibility values (here, F -values) because
 279 calculated susceptibility values do not have any statistical relationship with existing landslides
 280 (as they do in other statistical landslide susceptibility analysis techniques).
 281 To obtain the success rate curve for the F -values, the calculated index values of all pixels in
 282 the map were sorted in descending order. The ordered pixel values were subsequently
 283 categorised into 100 classes with 1% cumulative intervals and an F -value map was prepared
 284 using the slicing operation in ILWIS 3.3. The F -value map was crossed with the landslide
 285 inventory map and the success rate curve was prepared from cross table values.
 286 For the earthquake-induced landslide after Niigataken Chuetsu-oki Earthquake of 2007, the
 287 success rate reveals that in 10% of the study area, F -values had a high rank and could explain
 288 47.3% of total landslides. Likewise, 30% of higher landslide hazard index (LHI) values could
 289 explain 74.3% of all existing landslides. Fig. 6 provides percent coverage of landslides as a
 290 function of F -value. To compare the landslide susceptibility values, the area under the curves
 291 (Lee, 2004, Dahal et al., 2008a; Dahal et al., 2008b) were estimated from the success rate
 292 graphs (Fig. 6). The area under the curve qualitatively measures the success rate or prediction
 293 rate of the F -values. A total area equal to one denotes perfect prediction accuracy.
 294 Alternatively, when the area under the curve is less than 0.5000, the analysis is invalid. In this
 295 study, the area under the curve was 0.7814, indicating that the prediction rate was 78.14%
 296 (Fig. 6) and the analysis is valid.



297
 298 Figure 6. Success rate curve and prediction rate of susceptibility map for the selected sub-site.
 299 To construct the classified susceptibility map of the selected sub-site, the reference success
 300 rate curve (Figure 6) was created, and the corresponding F -values for susceptibility levels of

301 30%, 50%, 70% and 90% (with F -values ranging from low to high) were calculated. Five
302 landslide susceptibility classes were established: very low (less than 30%), low (30-50%),
303 moderate (50-70%), high (70-90%), and very high (more than 90%, i.e. the highest F -values).
304 The susceptibility map of the sub-site prepared based on these intervals is shown in Fig. 7.

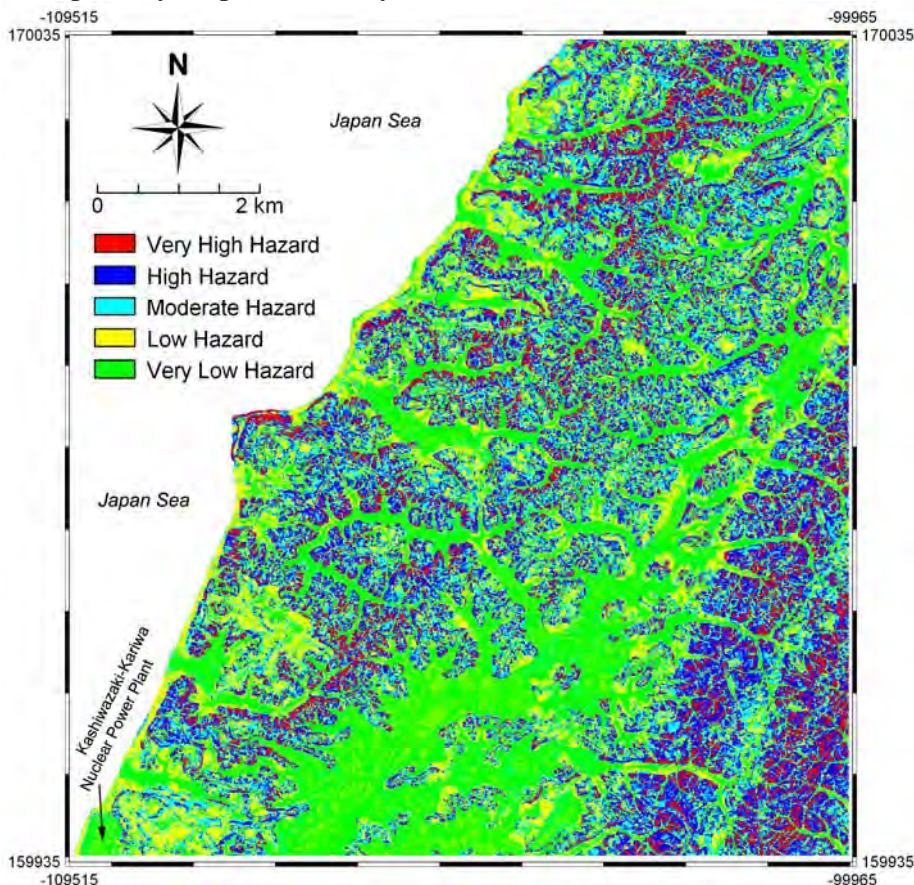


305
306 Figure 7. Susceptibility map of the selected sub-site of Kashiwazaki City. Landslides after the
307 Niigataken Chuetsu-oki Earthquake of 2007 are also shown on the map.

308 7 Discussions and final susceptibility map

309 The predictive power (81.5% accuracy, see Fig. 6) of the F -value calculated for the ideal sub-
310 site clearly suggests that the method proposed by Uchida et al. (2004) is reasonably accurate,
311 although few intrinsic parameters are used in the analysis and the method is absolutely
312 dependent on DEM. The success rate of landslide susceptibility and hazard analyses of both
313 rainfall-induced and earthquake-induced landslides generally ranges from 75% to 85%
314 (Chung and Fabbri 1999; Chung and Fabbri 2003; Lee, 2004; Lee and Talib 2005; Dahal et al.
315 2008a, b; Kamp et al. 2008; Yao et al. 2008). In such statistical analyses many intrinsic
316 parameters are necessary (for example, geology, slope aspect, soil depth, soil type, land use,
317 distance to road, distance to shore, distance to drainage, etc.), and data procurement can be
318 extremely challenging. However, the method proposed by Uchida et al. (2004) requires only

319 slope and curvature available from precisely-generated DEM data, and there is no need to
320 consider any other intrinsic parameters. The maximum ground acceleration from earthquake
321 shaking, which is site-specific, can be input as an approximation. Given the available data
322 from previous earthquakes in a particular area, the recorded or probable future maximum
323 ground acceleration can be used for susceptibility analysis in the area. In this work, a
324 susceptibility map with more than 81% accuracy was obtained using only three parameters.
325 This result is very encouraging, suggesting that the method proposed by Uchida et al. (2004)
326 is useful for evaluating the probability of earthquake-induced shallow landslides in any area.
327 The susceptibility analysis of the ideal sub-site served as a calibration of the method described
328 by Uchida et al. (2004) for the given maximum ground acceleration value. This finding was
329 extrapolated to obtain *F*-values for the whole study area (calculated in GIS), and a
330 susceptibility map for the entire region was prepared. The intervals of *F*-values used were the
331 same as for the sub-site (30, 50, 70, and 90%). The resultant earthquake-induced landslide
332 susceptibility map of the entire study area, given in Fig. 8, can be utilized for earthquake-
333 induced landslide susceptibility evaluation, planning, and preparation in the study area. The
334 geology and geomorphological setting of the sub-site and the entire region are similar, and the
335 final susceptibility map can be considered the most accurate earthquake-induced landslide
336 susceptibility map of the study area.



337
338 Figure 8. Final-DEM based earthquake-induced landslide susceptibility map of the
339 Kashiwazaki City area. Given the prediction rate of the susceptibility map of the sub-site (see
340 Fig. 6 and Fig. 7), the accuracy of this final susceptibility map is likely more than 80%.

341 **8 Conclusions**

342 Zoning of earthquake-induced landslide susceptibility is possible using the methodology of
343 Uchida et al. (2004) combined with GIS techniques. This study considered the concept of
344 seismic topographic amplification for a study area located in the Kashiwazaki, Niigata
345 prefecture of Japan, which was heavily hit by the Niigataken Chuetsu-oki Earthquake in 2007.
346 The effect of ground acceleration was employed on each cell in raster GIS. The primary
347 conclusion of this study is that precise DEM is adequate for the analysis of medium scale
348 earthquake-induced landslide susceptibility.

349 In an ideal sub-site within the study region, most of the slope pixels, which are indicated by
350 the landslide inventory map as landslide areas, are located just below the zones identified as
351 highly or very highly susceptible to landslides. The resultant susceptibility map of the ideal
352 sub-site shows more than 81.5% accuracy. Establishing on the high accuracy of the sub-site
353 analysis, a similar scheme for classifying for landslide susceptibility values was used for the
354 entire study area. As a result, the predictive power of the final susceptibility map for the
355 whole study region is likely around 80%. This map will prove useful for regional scale
356 planning.

357 **9 Acknowledgements**

358 We thank Mr. Anjan Kumar Dahal, Ms. Seiko Tsuruta and Mr. Toru Mimura for their
359 technical support during the preparation of this paper.

360 **10 References**

- 361
362 Ambraseys N, Srbulov M (1995) Earthquake induced displacement of slopes. *Soil Dyn.*
363 *Earthqu. Eng.* 14:59– 71
364 Bannister SC, Husebye ES, Ruud BO (1990) Teleseismic P coda analyzed by three-
365 component and array techniques: deterministic location of topographic P-to-Rg
366 scattering near the NORESS array, *Bull. seism. Soc. Am.* 80:1969-1986
367 Bouchon M, Schultz CA, Toksoz MN (1996) Effect of three-dimensional topography on
368 seismic motion”, *Journal of Geophysical Research* 101(B3): 5835-5846
369 Capolongo D, Refice A, Mankelov J (2002) Evaluating earthquake-triggered landslide hazard
370 at the basin scale through GIS in the upper Sele river valley, *Surveys in Geophysics* 23:
371 595–625
372 Carro M, De Amicis M, Luzi L, Marzorati S (2003) The application of predictive modeling
373 techniques to landslides induced by earthquakes: the case study of the 26 September
374 1997 Umbria-Marche earthquake (Italy), *Engineering Geology* 69 (1-2):139-159
375 Chávez-García FJ, Sanchez LR, Hatzfeld D (1996) Topographic Site Effects and HVSR, A
376 Comparison Between Observation and Theory, *Bulletin of the Seismological Society of*
377 *America* 86(5):1559-1573
378 Chigira M, Yagi H (2006) Geological and geomorphological characteristics of landslides
379 triggered by the 2004 Mid Niigata prefecture earthquake in Japan, *Engineering Geology*
380 82: 202-221

381 Chigira, M, Wang WN, Furuya T, Kamai T (2003) Geological causes and geomorphological
382 precursors of the Tsaoiling landslide triggered by the 1999 Chi-Chi Earthquake, Taiwan.
383 Engineering Geology 68: 259– 273

384 Chung C-JF, Fabbri AG (1999) Probabilistic prediction models for landslide hazard mapping.
385 Photogrammetric Engineering and Remote Sensing 65:1389-1399

386 Chung C-JF, Fabbri AG (2003) Validation of spatial prediction models for landslide hazard
387 mapping. Natural Hazards 30:451-472

388 Clouser RH, Langston CA (1995) Modeling observed P-Rg conversions from isolated
389 topographic feature near the NORESS array, Bull. Seism. Soc. Am. 85:195-211

390 Dahal RK, Hasegawa S, Nonomura A, Yamanaka M, Masuda T, Nishino K (2008a) GIS-
391 based weights-of-evidence modelling of rainfall-induced landslides in small catchments
392 for landslide susceptibility mapping, Environmental Geology 54 (2): 314-324

393 Dahal RK, Hasegawa S, Nonomura A, Yamanaka M, Dhakal S, Poudyal P (2008b) Predictive
394 modelling of rainfall induced landslide hazard in the Lesser Himalaya of Nepal based on
395 weights-of-evidence, Geomorphology (in press), doi: 10.1016/j.geomorph.2008.05.041.

396 Davis LL, West LR (1973) Observed effects of topography on ground motion. Bull. Seism.
397 Soc. Amer. 63:283-298

398 ERI (2007) Earthquake research institute Tokyo, Information available in [http://www.eri.u-](http://www.eri.u-tokyo.ac.jp/topics/20070716/)
399 [tokyo.ac.jp/topics/20070716/](http://www.eri.u-tokyo.ac.jp/topics/20070716/) access on 2008-3-10.

400 Gazetas G, Kallou PV, Psarropoulos PN (2002) Topography and soil effects in the MS 5.9
401 Parnitha (Athens) Earthquake: The case of Adámes, Natural Hazards 27: 133–169

402 Geli L, Bard PY, Jullien B (1988) The effect of topography on earthquake ground motion: a
403 review and new results, Bulletin of the Seismological Society of America 78(1):42-63

404 Gilbert F, Knopoff L (1960) Seismic Scattering from Topographic irregularities, Journal of
405 Geophysical Research 65: 3437-3444

406 Greenfield RJ (1971) Short-period P-wave generation by Rayleigh-wave scattering at Novaya
407 Zemlya. J. Geophys. Res.76: 7988–8002

408 Griffith DW, Bollinger GA (1979) The effect of Appalachian Mountain topography on
409 seismic waves, Bull. Seis. Soc. Am. 69:1081-1105

410 GSI (2007) Geographical Survey Institute, Topographic Map of Japan available in
411 <http://watchizu.gsi.go.jp> (accessed on 2007-11-13)

412 GSJ (2002) Computer graphics geology of the Japanese Islands, CD-ROM, Edited by the
413 editorial committee for the Geology of the Japanese Islands under the supervision of the
414 Geological Survey of Japan, Maruzen Co Ltd.

415 Harp EL, Jibson RW (1996) Landslides triggered by the 1994 Northridge, California
416 earthquake, Seismol. Soc. Am. Bull. 86(1B): S319–S332

417 Harp EL, Keefer DK (1990) Landslides triggered by the earthquake. In: Rymer MJ, Ellsworth,
418 WL (eds) The Coalinga, California, earthquake of May 2, 1983, U.S. Geological Survey
419 Professional Paper 1487: 335–347

420 ITC (2006) Integrated Land and Water Information System (ILWIS), a PC-based GIS and
421 Remote Sensing software Developed by International Institute for Geo-
422 Information Science and Earth Observation (ITC).

423 Jibson RW, Harp EL, Michael JA (1998) A method for producing digital probabilistic seismic
424 landslide hazard maps : An example from the Los Angeles, California Area, USGS
425 Open-File Rep: 98-113.

426 Jibson RW, Harp EL, Michael JA (2000) A method for producing digital probabilistic seismic
427 landslid hazard maps. *Engineering Geology* 58:271– 290

428 JMA (2007) Earthquake Disaster and Tsunami after Niigataken Chuetsu-oki Earthquake 2007,
429 Japan Meteorological Agency report, 60p, (in Japanese) available in home page
430 http://www.seisvol.kishou.go.jp/eq/2007_07_16_chuetu-oki/chuetsu-oki-saigai.pdf
431 accessed on 2008-01-25.

432 Kamp U, Growley BJ, Khattak GA, Owen LA (2008) GIS-based landslide susceptibility
433 mapping for the 2005 Kashmir earthquake region, Article in Press, *Geomorphology*
434 (2008), doi: 10.1016/j.geomorph.2008.03.003

435 Kawase H, Aki K (1988) Topography effect at the critical SV wave incidence: possible
436 explanation of damage pattern by to the Whittier-Narrows, California, earthquake of 1
437 October 1987, *Bull. Seism. Soc. Am.* 80:1-22

438 Kayen R, Collins B, Abrahamson N, Ashford S, Brandenberg SJ, Cluff L, Dickenson S,
439 Johnson L, Tanaka Y, Tokimatsu K, Kabeyasawa T, Kawamata Y, Koumoto H,
440 Marubashi N, Pujol S, Steele C, Sun JI, Tsai B, Yanev P, Yashinsky M, Yousok K
441 (2007) Investigation of the M6.6 Niigata-Chuetsu Oki, Japan, Earthquake of July 16,
442 2007, USGS Open File Report 2007–1365, p 230

443 Keefer DK (1984) Landslides caused by earthquakes, *Geol. Soc. Am. Bull.* 95:406–421

444 Keefer DK (2000) Statistical analysis of an earthquake-induced landslide distribution – the
445 1989 Loma Prieta, California event, *Engineering Geology* 58(3-4): 231-249

446 Khazai B, Sitar N (2003) Evaluation of factors controlling earthquake-induced landslides
447 caused by Chi–Chi earthquake and comparison with the Northridge and Loma Prieta
448 events. *Eng Geol* 71:79–95

449 K-Net (2008), Strong tremor by the Niigata Chuetsu-oki Earthquake, 2007 June 16, web page
450 http://www.k-net.bosai.go.jp/k-net/topics/chuetsuoki20070716/chuetsuoki_1.htm (accessed on
451 2008-08-07)

452 Tobishima Corporation (2008), Analysis of Niigata-ken Chuetsu-oki earthquake from K-net’s ground
453 motion data, available at [http://www.tobi- tech.com/lab/Bousai/20070716/2007chuetsuoki.pdf](http://www.tobi-tech.com/lab/Bousai/20070716/2007chuetsuoki.pdf)
454 (accessed on 2008-08-07) (in Japanese)

455 Kobayashi I, Tateishi M, Yoshimura T, Umemura T (1993), Geological Map of Japan,
456 1:50000, Izumozaki, Geological Survey of Japan.

457 Kobayashi I, Tateishi M, Yoshimura T, Ueda T, Kato H (1995), Geological Map of Japan,
458 1:50000, Kashiwazaki, Geological Survey of Japan.

459 Lee S (2004) Application of likelihood ratio and logistic regression models to landslide
460 susceptibility mapping in GIS. *Environ Manage* 34(2):223–232

461 Lee S, Evangelista DG (2006) Earthquake-induced landslide-susceptibility mapping using an
462 artificial neural network, *Nat. Hazards Earth Syst. Sci.* 6:687–695

463 Lee S, Talib JA (2005) Probabilistic landslide susceptibility and factor effect analysis.
464 *Environ Geol* 47:982–990

465 Lin C-W, Shieh C-L, Yuan B-D, Shieh Y-C Liu S-H Lee S-Y (2003) Impact of Chi-Chi
466 earthquake on the occurrence of landslides and debris flows: example from the
467 Chenyulan River watershed, Nantou, Taiwan, *Engineering Geology* 71:49-61

468 Luzi L, Pergalani F (1996) Application of statistical and GIS techniques to slope instability
469 zonation. *Soil Dyn. Earthqu. Eng.* 15(2): 83– 94

470 Luzi L, Pergalani F (2000) A correlation between slope failures and accelerometric
471 parameters: the 26 September 1997 earthquake (Umbria– Marche, Italy). *Soil Dyn.*
472 *Earthqu. Eng.* 20: 301–313

473 Mankelov JM, Murpy W (1998) Using GIS in the probabilistic assessment of earthquake
474 triggered landslide hazards, *Journal of Earthquake Engineering* 2(4):593-623

475 Miles SB, Keefer DK (2000) Evaluation of seismic slope-performance models using a
476 regional case study, *Environmental & Engineering Geoscience*, 6(1):25-39

477 Newmark NM (1965) Effects of Earthquake on Dams and Embankments, *Geotechnique*
478 15(2):139-159

479 Nishida T, Kobashi S, Mizuyama T (1997) DTM-based topographical analysis of landslides
480 caused by an earthquake, *Journal of Japan Society of Erosion Control Engineering* 49:9-
481 16 (in Japanese)

482 Ohtsuki A, Harumi K (1983) Effect of topography and subsurface inhomogeneities on seismic
483 SV waves, *Journal of Earthquake Engineering & Structural Dynamics* 11:441–462

484 Owen LA, Kamp U, Khattak GA, Harp EL, Keefer DK, Bauer MA (2008) Landslides
485 triggered by the 8 October 2005 Kashmir earthquake, *Geomorphology* 94:1–9

486 Parise M, Jibson RW (2000) A seismic landslide susceptibility rating of geologic units based
487 on analysis of characteristics of landslides triggered by the 17 January, 1994 Northridge,
488 California earthquake, *Eng. Geol.* 58:251–270

489 Takeuchi K, Kawabata D (2007) 1:50000 Digital geological map of Kashiwazaki-Higashi-
490 Kubiki region, Niigata Prefecture GSJ Openfile Report, No. 464, CD-ROM, Geological
491 Survey of Japan, AIST.

492 Trifunac MD (1973) Analysis of strong earthquake ground motion for prediction of response
493 spectra, *Earthquake Eng. and Struct. Dynam.* 2(1): 59-69

494 Uchida T, Kataoka S, Iwao T, Matsuo O, Terada H, Nakano Y, Sugiura N, Osanai N (2004) A
495 study on methodology for assessing the potential of slope failures during earthquakes.
496 Technical note of National Institute for Land and Infrastructure Management, p 91 (in
497 Japanese with English summary)

498 Uchida T, Osanai N, Onoda S, Takayama T, Tomura K (2006) A simple method of producing
499 probabilistic seismic shallow landslide hazard, In: Marui H, Marutani T, Watanabe N,
500 Kawabe H, Gonda Y, Kimura M, Ochiai H, Ogawa K, Fiebigler G, Heumader J, Rudolf-
501 Miklau F, Kienholz H, Mikos M (Eds.), *Proc. Interpraevent Int. Symp, Niigata 2006,*
502 *Disaster mitigation of debris flow, slope failures and landslides, vol. 2.* Universal
503 Academy Press, Tokyo, pp 529-534.

504 Umeda Y, Kuroiso A, Ito K, Ito Y, Saeki T (1986) High accelerations in the epicentral area of
505 the Western Nagana Prefecture, Japan, Earthquake of 1984, *J. Seism. Soc. Japan*
506 39:217-228

- 507 Van Westen CJ, Terlien MTJ (1996) An Approach Towards Deterministic Landslide Hazard
508 Analysis in GIS. A Case Study from Manizales(Colombia), *Earth Surface Processes and*
509 *Landforms* 21:853-868
- 510 Van Westen, CJ, Rengers N, Soeters R (2003) Use of geomorphological information in
511 indirect landslide susceptibility assessment. *Natural Hazards* 30:399-419
- 512 Wang HB, Sassa K, Xu WY (2007) Analysis of a spatial distribution of landslides triggered
513 by the 2004 Chuetsu earthquakes of Niigata Prefecture, Japan, *Nat Hazards* 41:43-60
- 514 Wang WN, Nakamura H, Tsuchiya S, Chen CC (2002) Distributions of landslides triggered
515 by the Chi-Chi earthquake in Central Taiwan on September 21, 1999, *Journal of the*
516 *Japan Landslide Society* 38(4): 318-326
- 517 Wang WN, Wu HL, Nakamura H, Wu SC, Ouyang S, Yu MF (2003) Mass movements
518 caused by recent tectonic activity: the 1999 Chi-Chi earthquake in central Taiwan, *The*
519 *Island Arc* 12:325-334
- 520 Wilson RC, Keefer DK (1985) Predicting areal limits of earthquake-induced landsliding. In:
521 Ziony JI (Ed.), *Evaluating Earthquake Hazards in the Los Angeles Region - An Earth-*
522 *science Perspective*, US Geol. Surv. Prof. Paper 1360, pp 316-345
- 523 Yao X, Tham LG, Dai FC (2008) Landslide susceptibility mapping based on Support Vector
524 Machine: A case study on natural slopes of Hong Kong, China, *Geomorphology*, (in
525 press), doi:10.1016/j.geomorph.2008.02.011